MEASUREMENT OF THE MAGNETIC MOMENT OF THE PROTON IN UNITS OF THE NUCLEAR MAGNETON

B. A. MAMYRIN and A. A. FRANTSUZOV

A. F. Ioffe Physico-technical Institute, Academy of Sciences, U.S.S.R.

Submitted to JETP editor July 22, 1964

J. Exptl. Theoret. Phys. (U.S.S.R.) 48, 416-428 (February, 1965)

A new technique is proposed for measuring the magnetic moment of the proton in units of the nuclear magneton, using a magnetic resonance mass spectrometer. The cyclotron frequency is measured in a single revolution of the ions in the apparatus; earlier techniques did not possess this advantage. The magnetic moment of the proton (without correction for diamagnetic shielding of hydrogen nuclei in water) is 2.79279 ± 2 nuclear magnetons. The spread of the measurements is equivalent to $\pm 3.5 \times 10^{-6}$ rms relative error. The total rms relative experimental error is $\pm 6 \times 10^{-6}$.

MOST fundamental constants of atomic physics—Avogadro's number, Planck's constant, the charge and mass of the electron etc.—are known at the present time to within a fraction of the order 10^{-5}. In the most accurate experiments these quantities are not, as a rule, measured independently, but in certain combinations. The aggregate of experimental data yields the entire system of fundamental constants only after mathematical treatment and adjustment for consistency. Changes and refinements of any one of the originally measured quantities will affect the entire system.

One of the important initial quantities included in the final determination of adjusted constants[1-4] is the magnetic moment of the proton in units of the nuclear magneton. Its value is obtained by measuring the spin procession frequency of protons f_n (the nuclear magnetic resonance NMR frequency) and their cyclotron frequency $f_{c.p}$ in the same magnetic field.[5-8] We here have

$$f_n = (\mu_p / \pi\hbar) H, \tag{1}$$

where μ_p is the magnetic moment of the proton and H is the magnetic field, and

$$f_{c.p} = eH / 2\pi m_p c \tag{2}$$

where m_p is the proton mass, e is the electron charge, and c is the velocity of light. The ratio of these frequencies is

$$\frac{f_n}{f_{c.p}} = \frac{\mu_p}{e\hbar/2m_p c} = \frac{\mu_p}{\mu_n} \tag{3}$$

which is the magnetic moment of the proton in units of the nuclear magneton $\mu_n = e\hbar/2m_p c$.

Since the frequency of spin precession can be measured very accurately, the principal experimental difficulties are incurred in measuring the cyclotron frequency of the proton. The two methods heretofore used for this purpose employed an omegatron and a decelerating cyclotron, respectively. In both methods the required high accuracy is attained by having ions perform a large number of revolutions in a magnetic field before entering a collector. Special precautions must be taken to prevent vertical scattering of the ions. For this purpose a trapping electric field is applied in the omegatron, and a mechanism of phase focusing during deceleration between the dees is used in the decelerating cyclotron. Phase focusing in the cyclotron is operative only at frequencies of the decelerating potential above the cyclotron frequency; the observed experimental peak is shifted relative to the latter frequency. The theoretical calculation of this shift requires certain simplifying assumptions; the experimental peaks behave somewhat differently from the theory. Consequently, cyclotron frequency can be determined in a decelerating cyclotron with $\sim 2 \times 10^{-5}$ accuracy.

The omegatron method suffers from the shortcoming that ions starting out at thermal velocities move through a considerable fraction of their entire paths at low energies. Their cyclotron frequency is strongly affected by radial electric fields induced by the trapping potential, by the space charge field, and by contact potential differences. The effects of these fields are taken into account by extrapolating the measurements obtained for different ion masses or different magnetic fields to zero mass or an infinite magnetic field, respectively. It is assumed that the field of

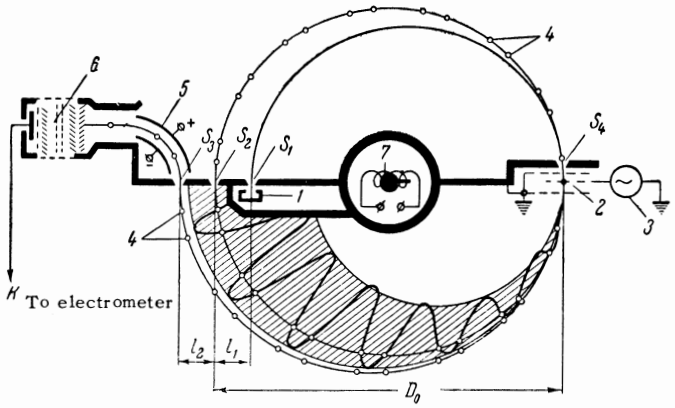

FIG. 1. Sketch of apparatus. 1 – Ion source, 2 – modulator, 3 – rf oscillator, 4 – ion bunches, 5 – extracting condenser, 6 – electron multiplier, 7 – NMR probe. D_0 = 224 mm; l_1 = 28 mm; l_2 = 26 mm; slits S_1, S_2, S_3, S_4 are 3 mm high and 0.2, 0.6, 0.4, and 0.5 mm wide, respectively. The 1300-Oe magnetic field is perpendicular to the plane of the drawing.

the space charge is not affected by changes in the operating conditions. However, this is not entirely accurate, and the omegatron is also limited to $\sim 2 \times 10^{-5}$ accuracy.

In our procedure for determining μ_p/μ_n the cyclotron frequency is measured with a magnetic resonance mass spectrometer. For a single revolution of ions in the magnetic field this instrument obtains narrower peaks of the output signal as a function of the frequency than were obtained by earlier techniques requiring many revolutions. The measurement of the cyclotron frequency during a single ion revolution represents an important advantage; the entire motion of an individual ion in the instrument is traced and a corresponding accurate theory can be constructed. In addition, when the trajectory of a single ion is known, accurate corrections can be introduced for the effects of perturbing electric fields and magnetic field inhomogeneities.

Our work began with the designing of a magnetic resonance mass spectrometer [9,10] as a basis for constructing the apparatus that will be described here. Measurement of the proton cyclotron frequency is not absolutely required for determining μ_p/μ_n. The measured cyclotron frequency of any other ion can be used in conjunction with the relation

$$f_{c.p} = f_c \frac{M}{q} \frac{1}{M_p}; \qquad (4)$$

here f_c is the cyclotron frequency of the ion, M is its mass, and q is its charge in elementary units. Since the mass ratios of light ions are known with greater than 10^{-6} accuracy,[11] no additional errors are introduced by the use of (4).

DESCRIPTION OF APPARATUS

Figure 1 is a sketch of the apparatus, having as its main part a magnetic resonance mass spectrometer [10] which operates as follows. Ions passing through the slit S_1 of the ion source are deflected by the magnetic field, perform a half revolution, and enter slit S_4 of the modulator. This part of the apparatus functions as a 180° static mass spectrometer possessing high enough resolution so that only ions of a single mass number enter slit S_4.

The modulator consists of three fine-gauge screen grids. The two outer grids are grounded; a sinusoidal voltage from a rf oscillator is applied to the central grid. Ions traversing the modulator receive a velocity increment which depends sinusoidally, in first approximation, on the instant of time when each ion passes through the central grid. Ions receiving different velocity increments move in orbits of different diameters; their positions at fixed instants are represented by the curve in the shaded region of Fig. 1. Slit S_2 is entered only by ions for which the increment of the diameter equals the distance l_1 between S_1 and S_2. Thus two short ion bunches emerge from S_2 during each period of the rf voltage applied to the modulator. After a half revolution the ions in these bunches again enter the modulator and receive a second velocity increment which depends on the ratio of their cyclotron frequency to the oscillator frequency. If

$$f_{osc} = nf_c, \qquad (5)$$

where n is an integer (usually about 200), ions pass through the plane of the central modulator grid at the time of their second acceleration in the same phase of the rf voltage as at the time of the first acceleration. In first approximation they receive the same velocity and diameter increments as at the first time. For $l_2 = l_1$ the ions enter exit slit S_3, are deflected in a cylindrical condenser, and enter the electron multiplier. The multiplier output current is amplified by an electrometer amplifier and is registered as the output current of the apparatus.

When the oscillator frequency is varied the ion bunches are gradually shifted away from slit S_3 and the output current vanishes. It can be shown [10] that the output current peak can be rendered very narrow as a function of frequency ($\Delta f/f$ = (25—30) $\times 10^{-6}$ at half-maximum). We note that the widths of the experimental peaks agree with the calcula-

tion in [10] and that their shapes exhibit no asymmetry. This indicates that the peak width depends entirely on the widths of the slits S_1, S_2, and S_3 and not on any other cause of defocusing. The resonance frequency $f_{osc} = nf_c$ can be determined to within a small fraction of the peak width. It is important to note that the cyclotron frequency is measured during a single ion revolution, from the first to the second passage through the modulator. This orbital trajectory will be called the operating orbit.

The foregoing simplified theory of the operation of our apparatus is valid for $l \ll D_0$. In our case $l_1/D_0 = 0.125$; the velocity increment is now not a strictly sinusoidal function of time and differs somewhat for the first and second accelerations within the modulator. In addition, the velocity increment differs for the first and second ion bunches formed during each rf period. If, nevertheless, both bunches are to impinge on the receiving slit for a single value of f_{osc}, a calculation shows that l_2 must be about 10% smaller than l_1. The apparatus permits variation of l_2; the receiving slit can be shifted during the time of operation to obtain peaks from both bunches for a single oscillator frequency f_{res}. This frequency was measured and was found to differ from that given by (5) as follows:

$$f_{res} = f_c(n + k); \tag{6}$$

here $k \ll 1$ and is independent of n.

In addition to the part played by the nonsinusoidal velocity increment, the correction k in (6) results from the accelerated ion motion on the small segment of its path inside the modulator, leading to a modification of the cyclotron period. In order to take these factors into account the exact equations of ion motion in the apparatus were written, assuming that a sinusoidal time-dependent force acts in the modulator regarded as a flat condenser. The calculation of k required the solution of six transcendental equations containing sines and cosines. This system of equations was solved numerically for parameters representing our operating conditions, yielding [1)]

$$k = -0.0028. \tag{7}$$

For this solution it was assumed that an ion traversed the modulator grid separation a during $^3/_4$ of a rf half-period. For n = 196 we obtain a = 1.35 mm; for n = 98 we have a = 2.70 mm.

In order to obtain a modulator that would represent the maximum approximation to an ideal flat capacitor we used fine-gauge copper screen grids manufactured electrolytically with square mesh openings of 125-μ sides separated by wires 7μ in diameter. The screens were stretched carefully and were plane parallel to within $\pm 4\mu$. The accuracy of the correction (7) can be established experimentally. From (6) we obtain

$$f_c = \frac{f_{res}}{n+k} \approx \frac{f_{res}}{n}\left(1 - \frac{k}{n}\right). \tag{8}$$

We thus have a correction k/n which differs in the measurements with different values of n; the correctness of the calculated value of k can thus be tested. With changes of n the separation of the modulator grids and the rf oscillator frequency must be varied in accordance with the foregoing discussion.

The design of the vacuum system, ion source, and modulator were described in [10] and were not changed. The operating parameters were changed in order to encompass lighter masses. Measurements were performed with He_4^+, Ne_{20}^{++}, and Ne_{20}^+ ions. The corresponding accelerating voltages in the source were 2000, 800, and 400 V; the cyclotron frequencies were 470, 158, and 94 kc, respectively.

The higher frequencies and voltages for lighter ions required the use of a new rf oscillator which could generate up to 1000 V at the modulator in the 10—100 Mc range.

All measurements were performed with minimum currents in order to avoid space charge effects. The louvered electron multiplier of 10^4 gain at the output enabled easy measurement of 10^{-15} A currents with a good signal-to-noise ratio.

The permanent magnet, which provided a field of 1300 Oe, was essentially the same as that described in [10]. We changed only the size of the shim rings mounted on the pole tips, and provided for the compensation of magnetic inhomogeneities resulting from nonuniform material of the pole tips.

The second and smaller portion of the apparatus consisted of a coil and ampoule at the center of the chamber, for detection of nuclear magnetic absorption signals. The ampoule was a sphere of 5 mm radius filled with a weak aqueous solution of $CuCl_2$. The coil was the inductive element of the oscillatory circuit located in one arm of the amplitude bridge.[12]

[1)]The authors greatly appreciate the assistance of N. V. Leont'eva, who solved the equations numerically.

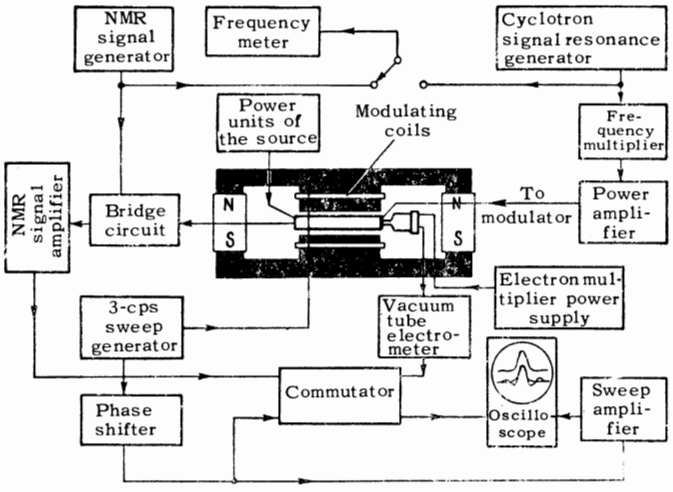

FIG. 2. Block diagram of apparatus for measuring the magnetic moment of the proton.

MEASURING TECHNIQUE AND SOME UNITS OF THE APPARATUS

The magnetic field in our apparatus is generated by a permanent magnet. However, we observed a temperature drift of the field and rapid jumps of the order $(2-5) \times 10^{-6}$, which were possibly caused by external magnetic fields. Thermostatic control as employed in [10] added a difficulty and did not exclude field jumps; we therefore employed a method of measurement that does not require rigid stabilization of the magnetic field. In this method the nuclear magnetic absorption signal and the current output peak of the magnetic resonance mass spectrometer were displayed simultaneously on the oscilloscope screen. Figure 2 is a block diagram of the apparatus enabling such observation. The magnetic field H is modified with a 3-cps frequency by a small sinusoidal field which is generated by special modulating coils bearing a current from a low-frequency oscillator. The oscilloscope sweep is driven by the voltage from the same oscillator, applied through a phase shifter and amplifier. The modulating magnetic field lags in phase behind the oscillator voltage because of Foucault currents in the material of the pole tips. The phase shifter adjusts the sweep phase to attain synchronous variation of the magnetic field in phase with the horizontal deflection of the oscilloscope beam. The sweep on the screen is calibrated in units of the magnetic field.

The cyclotron frequency varies proportionally to the magnetic field according to (2). The mass spectrometer output current appears whenever the cyclotron frequency passes through a value satisfying (6). This occurs for a magnetic field value H* which depends on the frequency f_{osc} of the voltage applied to the modulator. By varying f_{osc} we change H* and shift the signals along the horizontal axis of the oscilloscope.

The signal appears twice during each period, during the forward and reverse traces of the sweep. When the magnetic field varies in phase with the sweep, both signals appear at the same location on the screen and their contours are merged (Fig. 3a). With variation of the phase by the phase shifter, the two signals move in opposite directions on the screen (Fig. 3b), while their axis of symmetry remains undisplaced.

A nuclear magnetic absorption signal also appears twice during each period, i.e., whenever the magnetic field assumes a value for which the spin precession frequency coincides with the rf of the oscillator in the bridge. The NMR signal can also be shifted on the screen by varying the oscillator frequency.

In order to permit simultaneous observation, both signals are applied to the ÉNO-1 oscilloscope through a commutator which switches on the NMR signal during one trace of the sweep and switches the mass spectrometer signal during the next trace. The afterglow of the screen permits simultaneous observation of the two signals. If, now, when the frequency of one of the oscillators is varied, the axes of symmetry of the two signal images coincide on the screen (Fig. 3c), both signals are associated with the same magnetic field. The frequency ratio of the NMR and cyclotron resonance oscillators could be measured in such cases for the subsequent calculation of μ_p/μ_n.

Variation of the magnetic field when the oscil-

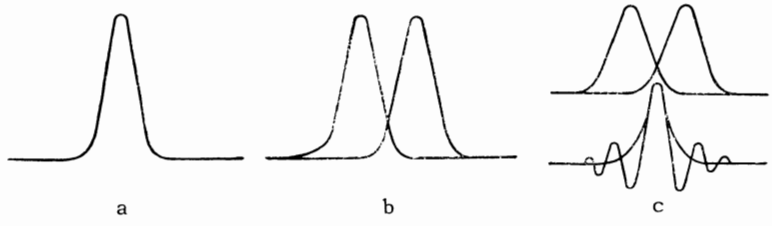

FIG. 3. Cyclotron resonance and nuclear magnetic absorption signals displayed on oscilloscope screen.

lator frequencies are correctly adjusted causes the signals to move together from the screen center towards one side, while their axes of symmetry continue to coincide. Observation of the coincident peaks on the screen monitors the invariance of the NMR and cyclotron resonance oscillators during the measurement of their frequency ratio.

The master oscillator frequencies were measured with a ChZ-4 frequency meter; two frequency meters were used in parallel, as a rule, to obtain reliable measurements. A frequency meter counts the number of periods of the measured frequency during one second. The second intervals are marked off by dividing a 100 kc frequency generated inside the instrument by a special thermostatically controlled quartz crystal oscillator. Since the frequency ratio of two oscillators was being measured, the final result does not include the absolute frequency of the crystal oscillator; only the (entirely adequate) stability of the latter was required. The NMR frequency was 5.23 Mc; the frequency of the mass spectrometer oscillator was in the range 4—6 Mc. Since the frequency meter measured frequencies to within ±1 cps, the accuracy of the frequency ratios was limited by the accuracy of peak coincidence and by the stability of the oscillators. Power was supplied to the plate-filament circuits of the two master oscillators from separate stabilized rectifiers, thus completely ensuring their required stability during the measurement period of a few seconds. The accuracy of the frequency ratio measurements therefore depended ultimately only on the preciseness of peak superposition on the oscilloscope screen.

The shape of the cyclotron resonance signal is shown in Figs. 3a, b. The signal-to-noise ratio varied from 10 to 20, depending on the operating conditions of the apparatus. The peak width at half-maximum for the master oscillator frequency was ~100—150 cps. The shape of the NMR signal is represented by the lower curve in Fig. 3c. Its signal-to-noise ratio was about 20, and the NMR half-maximum width was about 50 cps.

The accuracy of peak superposition (and at the same time the stability of the oscillators) was evaluated from the frequency variation required for a clearly observable relative displacement of the centers of symmetry of the two peaks. Repeated tests showed that frequency changes ≤ 10 cps were sufficient for this purpose. The accuracy of the ratio of the NMR and cyclotron resonance signals was thus estimated to be $\pm(1-2)\times 10^{-6}$.

In the foregoing method good transmission of the mass spectrometer signal requires a passband of about 60 cps for the electrometer amplifier. Our electrometer was similar to that described in [13].

In the entire foregoing discussion it was assumed that the magnetic field was homogeneous in the magnet gap, whereas in actuality the field along the operating orbit differs from the field at the center where the NMR probe is located. The discrepancies can be evaluated, as will now be shown, if we know the difference between the field at each point of the operating orbit and at the center. When these differences are measured in the case of an unstabilized magnet, good accuracy can be attained by the method of simultaneous display, with superposition (on the oscilloscope screen) of signals from two probes, on the orbit and at the center, respectively. For this purpose the NMR signal from each probe is observed by means of a separate bridge; the commutator feeds each signal alternately to the oscilloscope. A switch operating simultaneously with the commutator abruptly changes the circuit capacitance of the oscillator feeding both bridges. The oscillator frequency then changes in value by a jump which can be varied smoothly to bring about coincidence on the screen between the signals from the first and second probes. The difference between the magnetic fields at the locations of the two probes is derived from the formula

$$\Delta H / H = \Delta f / f, \tag{9}$$

where Δf is the jump of oscillator frequency. The circuit connections for measuring the field differences are similar, on the whole, to the block diagram Fig. 2.

CORRECTIONS AND ACCURACY OF RESULTS

Following the measurement of a cyclotron resonance frequency and NMR frequency the magnetic moment of the proton can be calculated on the basis of (3), (4), and (6). However, the value thus attained is subject to several corrections, which we shall now consider.

A. Correction for inhomogeneous magnetic field. Because of magnetic field inhomogeneity the frequency of ion revolution differs from the value corresponding to the field H_0 at the center of the chamber, where the NMR probe is located. It can be shown that this difference is given by

$$\frac{\Delta f_c}{f_c} = \frac{1}{2\pi H_0}\int_0^{2\pi} \Delta H(\Phi)\,(1-\cos\Phi)\,d\Phi = \frac{h}{H_0}. \tag{10}$$

Here $\Delta H(\Phi)$ is the difference between the fields at a given orbital point and at the center; Φ is the angular distance of this point from the modulator, and h is the equivalent correction of the magnetic field. Equation (10) shows that the correction h is the average difference between the field at the center and the field at orbital points weighted by $1 - \cos\Phi$. Equation (10) is correct to terms of the order $(\Delta H/H)^2$. Since $\Delta H/H$ equaled a few units of 10^{-5} in our magnet, the quadratic terms were negligible. Using the above-described technique of measuring $\Delta H/H$, we obtained h/H_0 with 2×10^{-6} accuracy.

The mass spectrometer chamber was made of nonmagnetic brass whose magnetic properties were carefully checked.[15] However, ΔH was measured inside the chamber with a movable NMR probe while the chamber was located in its working position relative to the magnet. In this way we took into account the possible magnetic field distortions resulting from paramagnetic material in the elements of the apparatus located within the chamber, or due to steel parts surrounding the chamber.

It was found that when the chamber is moved rapidly into the magnet gap, the field distribution in the gap is changed because of eddy currents generated in the material of the chamber. Although the eddy currents disappear rapidly, some remanent magnetization is found in the pole tips, and the field pattern along the orbit is changed. This effect was obviated by moving the chamber slowly into the gap at 1 mm/sec using a special motor drive. The field distribution in the gap changes very little with time; the change of h/H_0 was at most $(2-3) \times 10^{-6}$ during a measuring cycle.

The correction h/H_0 depends on the disposition of the orbit relative to the magnet; therefore the chamber always occupied an identical position in the gap to within 0.5 mm. The principal uncertainty regarding the location of the operating orbit resulted from the dimensions of the slits; the largest of these dimensions were the uniform slit height of 3 mm and the 5-mm width of the aperture slit (not shown in Fig. 1). Any displacement of the chamber from its customary operating position through these distances in the corresponding directions would shift the cyclotron frequency by less than $\pm 3 \times 10^{-6}$. It can therefore be assumed that we are able to evaluate the inhomogeneity of the field with better than 3×10^{-6} accuracy.

Magnetic field distortions generated by the cathode current in the ion source were evaluated by reversing the direction of this current and thus reversing the direction of the distortions. The correction was 2×10^{-6}.

We also attempted to observe the frequency shift of the NMR signal resulting from the presence of the paramagnetic salt $CuCl_2$ in the aqueous sample. However, an increase of the salt concentration by a factor of several times did not affect the observed signal frequency by as much as the fraction 10^{-6}.

B. Correction for the nonsinusoidal form of the ion velocity increment induced by the modulator. This correction has already been discussed and furnished the correction term k in (6). The voltage applied to the modulator was assumed to be strictly sinusoidal, whereas in reality an oscillator does not furnish a perfectly sinusoidal voltage. Although the circuit of the resonance output amplifier possesses a good quality factor, the second harmonic was detected and its effect was assessed from the shift of the observed ion peak when the final resonance circuit was detuned. The phase of the second harmonic could be shifted $\pm 90°$ relative to the first harmonic. The observed relative shift of the cyclotron resonance frequency was then $(2-3) \times 10^{-6}$.

C. Correction for perturbing electric fields in the chamber. This correction can be introduced if measurements for ions of different masses are performed. The electric fields result from contact potential differences, space charge, and other causes. These fields deflect the ions and change their cyclotron frequency somewhat; in our experiments the fractional change was about 10^{-5}. The change of cyclotron frequency is proportional to the force acting on the ions due to the weighted average of the fields along the orbit. A detailed calculation shows that

$$\frac{\Delta f_c}{f_c} = \frac{1}{F_0}\left[\frac{e}{2\pi}\int_0^{\pi} E_r(\Phi)\,(1-\cos\Phi)\,d\Phi + \frac{e}{2\pi}\int_0^{2\pi} E_\Phi(\Phi)\sin\Phi\,d\Phi\right]. \tag{11}$$

Here E_r and E_Φ are the radial and azimuthal components of the electric fields at an orbital point, Φ is the angular distance of this point from the modulator, $(1 - \cos\Phi)$ and $\sin\Phi$ are weight factors, and F_0 is the centripetal force of the magnetic field acting on an ion. The magnetic field and the orbital radius were constant under our experimental conditions; therefore larger ion masses necessarily entailed lower energies. From elementary considerations, $1/F_0$ is here proportional to M/q of an ion. Consequently, Eq. (11) shows that the relative shift of cyclotron fre-

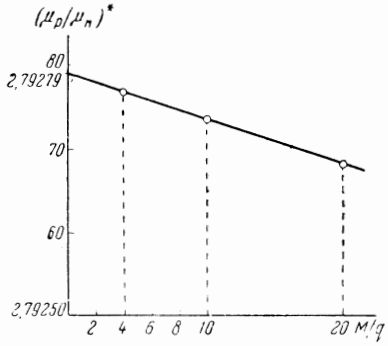

FIG. 4. An example of the correction for perturbing electric fields. The experimental points pertain to the ions He_4^+, Ne_{20}^{++}, and Ne_{20}^+.

quency resulting from the electric fields increases linearly with M/q if these electric fields do not vary [i.e., the expression within the square brackets of (11) remains constant]. Thus

$$\Delta f_c / f_c = AM / q, \tag{12}$$

where A is a constant depending only on the magnitude of the electric fields under our conditions. From (11) and (1), considering that $AM/q \ll 1$, we obtain

$$\frac{\Delta(\mu_p/\mu_n)}{\mu_p/\mu_n} = -A\frac{M}{q}; \tag{13}$$

here

$$\Delta\left(\frac{\mu_p}{\mu_n}\right) = \left(\frac{\mu_p}{\mu_n}\right)^* - \frac{\mu_p}{\mu_n}, \tag{14}$$

μ_p/μ_n is the true value of the proton magnetic moment in units of the nuclear magneton, and $(\mu_p/\mu_n)^*$ is the experimental value. From (13) and (14) we have

$$\left(\frac{\mu_p}{\mu_n}\right)^* = \frac{\mu_p}{\mu_n}\left(1 - A\frac{M}{q}\right). \tag{15}$$

This shows that the experimental values of $(\mu_p/\mu_n)^*$ depend linearly on M/q. The intersection of the corresponding straight line with the vertical axis gives the true value of μ_p/μ_n, and the slope of the line is proportional to the magnitude of the electric fields. The results of one set of measurements are shown in Fig. 4.

The foregoing method of introducing a correction for the effect of electric fields is valid only if these fields remain constant when the apparatus is retuned for differention masses. A number of control experiments were performed to test this important assumption. All high-voltage electrodes in the chamber were carefully shielded from the operating orbit. Nevertheless, it was verified separately that changes of the potentials of these electrodes do not affect the cyclotron frequency.

The field of ion space charge differs, as a general rule, for different values of M/q. However, it was shown experimentally that a fivefold increase of ion current above the customary operating condition did not induce a cyclotron frequency shift that could be detected within the accuracy limits of our measurements. This shows that the space charge field in the apparatus is negligibly small.

When the screen surfaces are bombarded with ions the so-called polarization potentials appear,

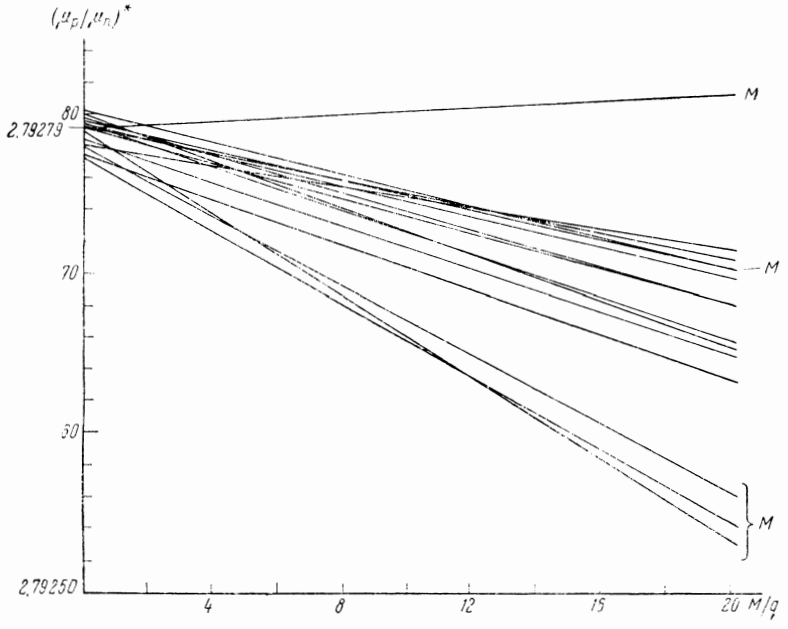

Fig. 5. Measurements of the magnetic moment of the proton in units of the nuclear magneton. The letter M designates measurements performed with pure copper screens.

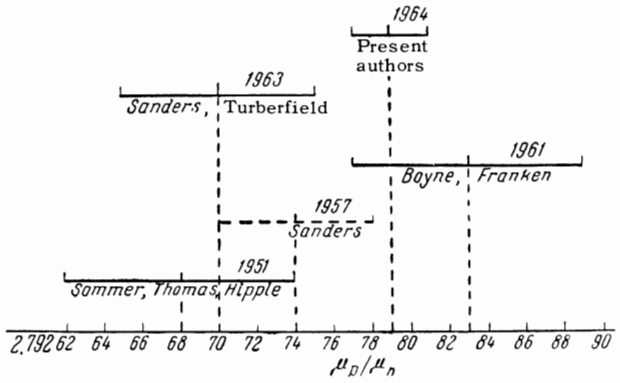

FIG. 6. Measurements of μ_p/μ_n reported by different authors.

which result from the charging of the dielectric surface films. In order to eliminate this effect the surfaces of all internal copper screens were carefully cleaned by chemical etching. In a control experiment some measurements were performed using screens covered with aquadag. These measurements and those from the pure copper screens coincided, as is shown in Fig. 5. It was thus confirmed that the polarization potentials, which should differ on the unlike surfaces, do not play an important role. This conclusion is also supported by the aforementioned experiment in which the operating current was increased.

RESULTS

Figure 5 presents the results of proton magnetic moment measurements obtained during a period of several months with n = 196. The plotted points represent values of μ_p/μ_n following all corrections except the correction for perturbing electric fields. This last correction for measurements during a single day is performed graphically on Fig. 5, so that the points on the ordinate axis will represent the corrected values of μ_p/μ_n.

We performed four sets of measurements. In each cycle we first measured the magnetic field distribution, then a series of μ_p/μ_n values, and finally repeated the magnetic field measurements.

Our final results were $\mu_p/\mu_n = 2.79279$ without correction for the diamagnetic shielding of the proton in water. A control run with n = 98 using a wider modulator yielded the same result to within 2×10^{-6}. The spread of the results gives an rms error of 3.5×10^{-6}. We must add to this the uncertainty 3×10^{-6} of the correction for magnetic field inhomogeneity, the possible error 3×10^{-6} due to oscillator harmonics, and the correction 2×10^{-6} for the uncertainty of k due to the microoptics of the grids. The total rms relative error is thus 6×10^{-6} and our result becomes

$$\mu_p / \mu_n = 2.79279 \pm 0.00002. \tag{16}$$

Figure 6 shows the measured values of μ_p/μ_n that have been reported beginning in 1951. The values are split into two groups; our result agrees well with that of Boyne and Franken,[7] but differs from that of Sommer, Thomas, and Hipple [5] and the later measurement by Sanders and Tuberfield [8] by approximately twice the error of the latter. We thus suspect the presence of systematic errors in connection with one of the results. We have carefully searched for the possible sources of such errors in our own procedure by performing the control experiments already described, as well as other additional geometric, magnetic, and electric checking measurements. We were unable to discover any cause of such a large systematic error.

We note in conclusion that the described technique for determining μ_p/μ_n using a magnetic resonance mass spectrometer permits the attainment of still higher accuracy than in our present work. This will require improved homogeneity of the magnetic field and the elimination of harmonics in the voltage applied to the modulator. It also appears that higher ion energies should reduce the spread of the direct measurements.

In conclusion the authors wish to thank N. I. Ionov, in whose laboratory this work was done, for his support, advice, and valuable discussions during all stages of the work. The authors also wish to thank V. A. Zagulin, who participated in the designing of the electronic apparatus, and B. N. Shustrov for many useful discussions.

[1] J. W. M. Du Mond and E. R. Cohen, Revs. Modern Phys. **25**, 691 (1953).

[2] Cohen, Du Mond, Layton, and Rollett, Revs. Modern Phys. **27**, 363 (1955).

[3] J. A. Bearden and J. S. Thomsen, Nuovo cimento **5**, Suppl. **2**, 267 (1957).

[4] Bur. Standards Tech. News Bull. **47**, 175 (1963).

[5] Sommer, Thomas, and Hipple, Phys. Rev. **82**, 697 (1951).

[6] J. H. Sanders, Nuovo cimento **6**, Suppl. **1**, 242 (1957).

[7] H. S. Boyne and P. A. Franken, Phys. Rev. **123**, 242 (1961).

[8] J. H. Sanders and K. C. Turberfield, Proc. Roy. Soc. (London) **A272**, 79 (1963).

[9] Ionov, Mamyrin, and Fiks, ZhTF **23**, 2104 (1953).
[10] B. A. Mamyrin and A. A. Frantsuzov, PTÉ No. 3, 114 (1962).
[11] König, Mattauch, and Wapstra, Nuclear Phys. **31**, 1 and 18 (1962).
[12] Yu. S. Egorov and G. D Latyshev, PTÉ No. 2, 80 (1956).
[13] A. V. Parshin and L. B. Ustinova, PTÉ No. 3, 102 (1964).

Translated by I. Emin
56